

ON MELT LAYER STABILITY FOLLOWING A PLASMA DISRUPTION

W.G. WOLFER and A.M. HASSANEIN

Fusion Engineering Program, Nuclear Engineering Department University of Wisconsin, Madison, Wisconsin 53706, USA

When hard plasma disruptions produce melting of a surface layer on first wall components, the melt layer is in general also subject to various forces. Among these, the forces produced by eddy currents and the magnetic fields are the most severe, and they may cause the removal of the melt layer. It appears that one of the most effective mechanisms for removal is by a Rayleigh–Taylor instability. Numerical results are presented for both the most critical wavenumber and its amplification exponent as a function of two parameters which account for the effect of viscosity and surface tension. The results given for the critical amplification exponent allow an easy assessment of the stability of a melt layer when the forces are known. Examples of such an assessment are given, and it is found that within the range of estimated eddy-current forces, the melt layer may or may not be stable. Hydrodynamic instabilities induced by flow and tangential forces appear to be less severe than the Rayleigh–Taylor instability.

1. Introduction

Plasma disruptions in near-term tokamak devices can deliver a sufficient amount of energy to sections or components of the first wall that melting and vaporization may occur. The possibility for melting and the time sequence of melt layer formation and resolidification has been analyzed in great detail recently [1,2]. The emphasis of the previous studies was particularly on evaporation [1] and on the melt layer thickness and melt duration [2]. In assessing the consequences and damage to the component exposed to the plasma disruption, it is usually assumed that the melt layer will stay in place and resolidify. Accordingly, only the evaporation leads to a permanent loss of material and contributes to the wall erosion in addition to sputtering. There are, however, other consequences of a hard plasma disruption aside from the thermal response of the wall.

Large transient thermal stresses are generated in the part of the wall which remains solid. Because of the accompanying high temperatures, these stresses will quickly relax and, upon cooling, large and opposite residual stresses will remain in the wall. An analysis of this problem is given in [3].

The other consequence of a plasma disruption is that eddy currents are induced in the first wall as the plasma current decays. Their interaction with the magnetic fields can cause sufficiently large forces on the first wall and the melt layer that the liquid may be removed before it can solidify.

The present paper deals with this latter possibility

utilizing the results in [2] for the melt layer evolution and its duration. A critical issue in assessing the melt layer stability is the magnitude, direction, and time dependence of the forces generated by the eddy currents. As the discussions in §2 will show, it is not possible to evaluate these forces precisely for the general case, as they depend critically on the detailed eddy-current pattern, on the time dependence of the plasma current decay, on the wall resistance, inductances, etc. Without a detailed specification of the wall configuration, the forces can only be estimated within a large range of possible values.

The melt layer removal may take various forms such as run-off, shake-off, and formation of various instabilities. In the present paper we shall consider the possibility of a Rayleigh–Taylor instability when the melt layer is subject to magnetic forces perpendicular to the melt surface and directed into the plasma chamber. Run-off at the edge of a component could be a serious problem also when the tangential magnetic forces are large. Vibrations induced by the plasma disruption could shake off the melt layer as well. The latter two possibilities are, however, even more design dependent than the possibility of a Rayleigh–Taylor instability.

2. Forces

The decay of the toroidal plasma current I_t induces eddy currents in the metallic components of the first wall. These eddy currents interact with the toroidal and

vertical magnetic fields, producing both tangential and normal forces on the first wall components. The penetration depth for the eddy current after a time t is of the order of $2(\mu_0\sigma t)^{1/2}$, where μ_0 is the magnetic permeability and σ is the electrical conductivity. After 1 ms, the penetration depth is about 5 cm for stainless steel and 1 cm for molybdenum. We may therefore assume that the eddy currents are uniformly distributed throughout the first wall by the time a melt layer has been formed. The distribution and pattern of the eddy currents depends on the detailed shape, orientation, and on the insulating barriers of the components of the first wall. A general expression can therefore not be given for the eddy currents. Nevertheless, in order to obtain a reasonable estimate of the magnitude of the electromagnetic loads, the recent analysis of Mast and Preis [4] can be used as a guideline.

The eddy currents induced in the poloidal direction and interacting with the toroidal field B_t produce a pressure normal to the wall whose average value along the toroidal circumference of the vessel is approximately given by

$$p = \frac{\delta\phi B_t^2}{\mu_0\phi_0} \frac{\exp(-t/\tau_{cd}) - \exp(-t/\tau_w)}{(\tau_{cd}/\tau_w) - 1}, \quad (1)$$

where ϕ_0 is the toroidal magnetic flux in the absence of the plasma, $\delta\phi$ is the diamagnetic flux change produced by the plasma, μ_0 is the magnetic permeability, τ_{cd} is the plasma current decay time, and τ_w is the eddy current decay time, assumed to be larger than τ_{cd} . Its exact value depends on the electrical resistivity of the wall material and on the mutual inductance of the various eddy-current circuits. The diamagnetic flux $\delta\phi$ is approximately given by

$$\delta\phi = \frac{\mu_0^2}{8\pi} \frac{1 - \beta_p}{\bar{B}_t} I_t^2, \quad (2)$$

where the poloidal β_p is the ratio of the plasma pressure and the magnetic pressure produced by the poloidal field B_p . \bar{B}_t is the average toroidal field, whereas the value B_t in eq. (1) is to be taken at the selected wall position. Its maximum value B_t^{\max} occurs on the in-board side of the first wall. Note that $\phi_0 = A\bar{B}_t$ where A is the plasma cross-section. For a near-term tokamak reactor such as INTOR, the plasma parameters are of the magnitude shown in table 1.

In a worst-case situation, when $\tau_{cp} \ll \tau_w$, the transient electromagnetic pressure on the wall as caused by the poloidal eddy currents could be as high as about 1 MN m⁻². Segmentation of the first wall can of course reduce the eddy current decay time so that τ_{cp} and τ_w

Table 1
Typical plasma parameters for a tokamak reactor

| Parameter | Value |
|------------------------|------------------|
| I_t | 7 MA |
| β_p | 3 |
| A | 6 m ² |
| B_t^{\max}/\bar{B}_t | 1.5 |

become more similar in magnitude. As a result, more realistic values for p are lower by at least an order of magnitude. Assuming a wall thickness of 1 cm, the electromagnetic forces per unit volume are then of the order of 10 MN m⁻³. Upper and lower values differing by one order of magnitude from this value cover then the possible range of eddy-current forces.

Other forces which could cause melt removal are smaller than the above forces. For example, the gravitational force on stainless steel is 0.07 MN m⁻³. When evaporation occurs, a recoil pressure is exerted on the molten layer. This recoil pressure is of the order of the equilibrium vapor pressure. At a typical maximum surface temperature of 3000 K reached during a hard disruption, this vapor pressure is about 0.05 MN m⁻² for stainless steel.

3. Rayleigh–Taylor instability

On those locations where the eddy-current forces point into the plasma, the molten layer is subject to possible Rayleigh–Taylor instabilities. This type of instability occurring at the surface of a liquid layer has been studied in the past for both semi-infinite [5,6] and finite fluid layers [7,8]. Of particular relevance are the latter two references. Feldman [7] has treated Rayleigh–Taylor instabilities of melt layers on ablating bodies on re-entry into the atmosphere and subjected to deceleration forces, when the viscosity in the fluid layer is either constant or exponentially increasing with depth. Liquid metals do exhibit a temperature-dependent viscosity according to the equation [9]:

$$\eta(T) = 5.7 \times 10^{-4} T_m^{1/2} M^{-1/6} \rho_l^{-2/3} * \times \exp[E_v(1/RT - 1/RT_m)] \quad (3)$$

where the viscosity is given in poise, T_m is the absolute melting temperature, M is the molecular or atomic weight, and ρ_l is the liquid density. When the activation

energy E_v is unknown, it can be reliably estimated with the empirical formula [9]:

$$\log E_v (\text{kcal}) = 1.36 \log T_m - 3.418 \tag{4}$$

in the case of metals.

For the temperature variations encountered in molten layers produced by plasma disruptions [1,2] the viscosity varies typically by a factor of 2–4. Only when excessive melting occurs at very high disruption energy fluxes will the viscosity variation through the melt layer resemble more the exponential increase with depth.

The effect of the surface tension is to help stabilize any disturbance of the liquid surface. For accurate results, it is then important to utilize a temperature-dependent surface tension

$$\sigma(T) = \sigma(T_m) + (d\sigma/dT)(T - T_m). \tag{5}$$

Values for both the liquid surface tension at the melting point, $\sigma(T_m)$, and the usually negative temperature coefficient $(d\sigma/dT)$ have been compiled by Murr [10].

Because of the minor variation in viscosity across the melt layer, the values chosen for both η and σ were always for the surface temperature. Although an average value of η for the entire melt layer would perhaps be more appropriate, the present choice is more conservative.

With the assumption of uniform viscosity, the Rayleigh–Taylor instability of a liquid layer is determined by the following equation obtained from the derivation of Feldman [7]:

$$\begin{aligned} D(\alpha, \beta) &= 4\alpha^2\beta(\alpha^2 + \beta^2) - (\alpha^2 + \beta^2) \\ &\times (\beta \cosh \alpha \cosh \beta - \alpha \sinh \alpha \sinh \beta) \\ &- 4\alpha^3\beta(\alpha \cosh \alpha \cosh \beta - \beta \sinh \alpha \sinh \beta) \\ &+ \alpha \bar{R}^2(1 - \alpha^2/\bar{W}) \\ &\times (\beta \sinh \alpha \cosh \beta - \alpha \cosh \alpha \sinh \beta) = 0. \tag{6} \end{aligned}$$

Note that this equation is of a different form than the corresponding one in Feldman’s paper.

This equation represents the dispersion relationship for surface waves of the form $\exp(ikx + \kappa t)$, where the wavenumber $k = 2\pi/\lambda$ is related to the parameter α by $\alpha = hk$ (7)

and the amplification exponent κ is related to β according to

$$\beta^2 = \alpha^2 + (h\rho_1/f)\kappa\bar{R}. \tag{8}$$

Here, h is the melt layer thickness, f the force density, and

$$\bar{R} = (f\rho_1)^{1/2}h^{3/2}/\eta \tag{9}$$

is the surface Reynolds number. It incorporates the effect of the viscosity on the melt layer stability, whereas the surface Weber number

$$\bar{W} = fh^2/\sigma \tag{10}$$

is a measure of the surface tension effect.

The dispersion relationship (6) yields the following results. As the wavelength λ of the disturbance increases or the wavenumber α decreases, the amplification decreases also. Furthermore, when α approaches $W^{1/2}$, the exponent κ drops precipitously to zero. Therefore, disturbances with a long wavelength or with a wavelength shorter than $2\pi(\sigma/f)^{1/2}$ are stable. Intermediate wavelengths may give unstable waves whose amplitude grows initially as $\exp(\kappa t)$.

In order to find the critical wave with the maximum value κ_c of the amplification exponent, a numerical search algorithm was used to deal with the extremely nonlinear equation $D(\alpha, \beta) = 0$. The results for both the critical wavenumber α_c and its corresponding critical exponent κ_c are shown in figs. 1 and 2, respectively.

Fig. 1 shows that disturbances with small wavenumbers are influenced only by the Weber number \bar{W} . When the surface tension is high, or the melt layer thickness small, or the forces very low, the surface tension controls the instability. However, when the Weber number \bar{W} increases, viscosity exerts a large influence on the instability as shown by the marked dependence on the Reynolds number \bar{R} . In fact, when this number becomes small as viscosity increases, the critical wavenumber becomes independent of \bar{W} above values of $\bar{W} = 10$. Similar trends are reflected also in the

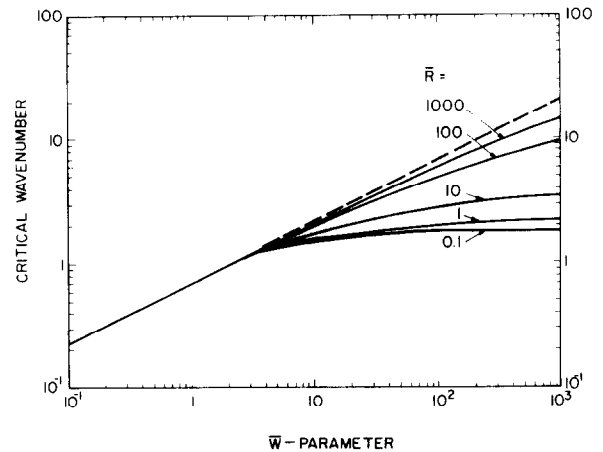


Fig. 1. Variation of the critical wavenumber with surface Weber number.

dependence of the critical exponent κ_c on the two parameters \bar{R} and \bar{W} . For large values of $\bar{W} > 10$ and small values of $\bar{R} < 10$, κ_c is nearly independent of \bar{W} and hence the surface tension. Conversely, when \bar{R} is large, κ_c depends mainly on \bar{W} .

Fig. 2 contains additional results of Feldman when the viscosity increases exponentially with depth. These results are shown as dashed lines, and have been obtained only for small values of the critical amplification exponent. The characteristic melt layer dimension in this case is the distance δ over which the viscosity increases e-fold, and the Reynolds and Weber numbers are now

$$R = (f\rho_1)^{1/2} \delta^{3/2} / \eta \quad \text{and} \quad W = f\delta^2 / \sigma. \quad (11)$$

We find that the results for the variable-viscosity case show the same dependence as the results for constant viscosity, at least within the parameter range where both cases have been evaluated. In fact, the dashed lines coincide with curves corresponding to those for constant viscosity when δ is replaced by

$$\delta = (2/5)^{4/7} h.$$

A thick melt layer with exponentially increasing viscosity is therefore equivalent to a melt layer of constant viscosity and a thickness of 1.6881δ . It remains to be investigated, however, if this equivalence can also be applied to melt layers with larger surface Reynolds and Weber numbers.

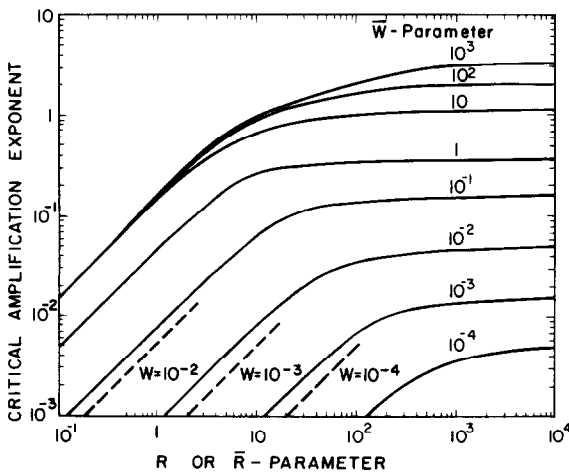


Fig. 2. Variation of the critical amplification exponent with surface Reynold's number.

4. Application to melt layers

During the course of a plasma disruption which results in surface melting, the surface temperature T_v , the melt layer thickness h , as well as the eddy-current forces f change continually with time. Therefore, when assessing the stability of a melt layer, two conditions must also be continually examined: first, the critical exponent $\kappa_c(t)$ must be evaluated at each point in time based on the present values of $T_v(t)$, $h(t)$, and $f(t)$. Second, the amplitude factor $\exp[\kappa_c(t)(t_{res} - t)]$ should remain of the order of one for the remainder of the melt duration $(t_{res} - t)$, where t_{res} is the time elapsed between the beginning of melting and the end of resolidification.

Instead of imposing a limit on the amplitude factor, we may also require that

$$\kappa_c(t)(t_{res} - t) \lesssim 1$$

as a condition for stability. In the following we shall use the term marginal stability whenever $\kappa_c(t)(t_{res} - t)$ is of the order of one, and unstable when this number greatly exceeds one.

As an intermediate step for the evaluation of $\kappa_c(t)$, the parameters \bar{R} and \bar{W} must be computed. Using the results of [2], the quantities $\bar{R}/f^{1/2}$ and \bar{W}/f are obtained and shown in figs. 3 and 4. The shape and time

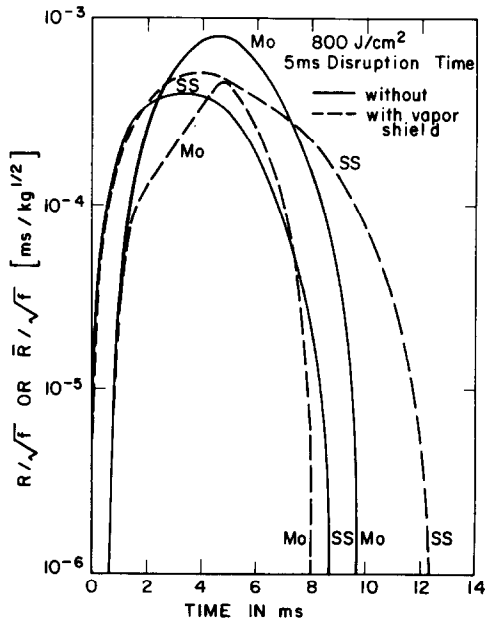


Fig. 3. Time variation of $R/f^{1/2}$ for 800 J cm^{-2} and 5 ms disruption time.

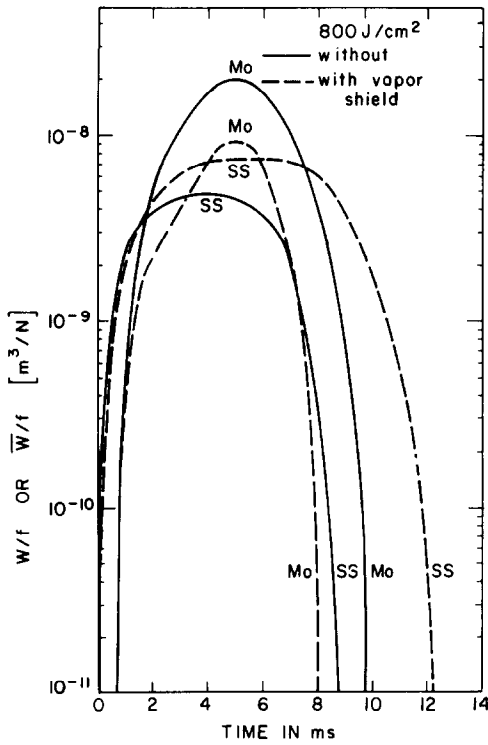


Fig. 4. Time variation of W/F for 800 J cm^{-2} and 5 ms disruption time.

variation of these curves is mainly determined by the corresponding variation of the melt layer thickness $h(t)$, and only to a minor degree by the temperature dependence of the viscosity and the liquid surface tension.

Since neither the precise magnitude nor the time dependence of the electromagnetic forces is known, a detailed stability analysis of the melt layer as a function of time is not warranted. Instead, we consider only the instability when the melt layer has its maximum thickness, and hence, the parameters $\bar{R}/f^{1/2}$ and \bar{W}/f assume their greatest values. Using again the results of [2], the maximum parameters are listed in table 2. Based on these values and using the results of fig. 2, the critical exponents κ_c are evaluated for three different values of the electromagnetic force, namely 1, 10, and 100 MN m^{-3} .

If we assume that the melt layer has a remaining life of about 3 ms, then $\kappa_c(t_{\text{res}} - t)$ are given by the last three columns of table 2. It is seen that the magnitude of the electromagnetic force has a decisive influence on the critical exponent. On the other hand, the value of the energy deposited has only a secondary effect as long as it results in a maximum melt layer thickness of the same order of magnitude.

It can be concluded that the melt layer remains stable for the lower value of the electromagnetic force, i.e. for 1 MN m^{-3} . Marginal stability or approaching instability is obtained for medium value of the force, 10 MN m^{-3} , whereas melt removal is certainly indicated for the highest values of the electromagnetic force of 100 MN m^{-3} .

Table 2
Melt layer parameter for a 5 ms plasma disruption

| Energy (J cm^{-2}) | Vapor shielding | Material | Max. melt thickness (μm) | $\bar{R}/f^{1/2}$ ($10^{-4} \text{ ms kg}^{-1/2}$) | \bar{W}/f ($10^{-9} \text{ m}^3 \text{ N}^{-1}$) | $\kappa_c(t_{\text{res}} - t)$ | | |
|----------------------------------|--------------------|----------|---|---|---|--------------------------------|------|------|
| | | | | | | 1 | 10 | 100 |
| 400 | yes | SS | 109 | 1.8 | 7.3 | 0.03 | 1.08 | 10.3 |
| | no | SS | 109 | 2.9 | 8.4 | 0.08 | 1.30 | 10.3 |
| 800 | yes | SS | 106 | 1.9 | 7.4 | 0.05 | 1.10 | 9.75 |
| | no | SS | 80 | 1.5 | 4.3 | 0.03 | 0.95 | 9.21 |
| 1200 | yes | SS | 93 | 2.6 | 7.1 | 0.07 | 1.17 | 10.1 |
| | no | SS | 60 | 1.0 | 2.5 | 0.02 | 0.73 | 8.79 |
| 400 | yes | Mo | 78 | 6.2 | 2.3 | 0.006 | 0.47 | 6.33 |
| | no | Mo | 90 | 8.3 | 3.1 | 0.01 | 0.52 | 6.51 |
| 800 | yes | Mo | 142 | 2.3 | 10 | 0.08 | 1.15 | 9.12 |
| | no | Mo | 188 | 4.0 | 19 | 0.10 | 1.36 | 11.3 |
| 1200 | yes | Mo | 186 | 3.8 | 18 | 0.09 | 1.29 | 10.9 |
| | no | Mo | 183 | 3.3 | 17 | 0.09 | 1.27 | 9.9 |

5. Discussion

The electromagnetic forces on the melt layer due to eddy currents appear to be large enough to cause melt removal by a Rayleigh–Taylor instability. The present work shows, however, that melt removal can be avoided by proper design such that the eddy-current decay constant is of similar order of magnitude to the plasma current decay time in a hard disruption. It appears then that with appropriate designs, the eddy-current forces can be minimized and the Rayleigh–Taylor instability can be avoided. The analysis presented in this paper can be easily extended to perform a step-by-step instability assessment when both the surface temperature, the melt layer thickness, and the eddy-current forces are known as a function of time. If the eddy currents peak before the melt layer has fully formed or after it has resolidified to a large extent, then melt removal can again be avoided even though the maximum eddy-current forces could be large. The present model together with the previously developed code for computing melting and evaporation [1,2] can provide an important design tool for limiters and first wall components.

In the above analysis of the melt layer stability we have only considered the component of the eddy-current forces perpendicular to the wall surface. Tangential components will, however, be present as well. This component will induce a flow of the melt layer similar to the flow of a liquid layer on an inclined plane. Hydrodynamic instabilities are known to occur when the Reynolds number $R' = \dot{M}/\eta$ exceeds a critical value; here, \dot{M} is the mass flow rate per unit span of the stream.

A limited investigation of this particular hydrodynamic instability has been carried out by Benjamin [11] for small Reynolds number R' and for a liquid layer in uniform laminar flow running down an inclined plane. If we apply his analysis to our present situation we find that the critical amplification exponent for this flow instability is given by

$$\kappa_c^f = \frac{\rho_1 f h^3}{3\eta^2} \sin \theta \left(\frac{8}{5} - \frac{2\eta}{\rho_1 h} \cot \theta \right)$$

where θ is the angle between the force per unit volume acting on the liquid and the surface normal. For a tangential load, $\theta = \pi/2$, and the critical exponent is found to be

$$\kappa_c^f = \frac{1}{3}(8/5)^2 \bar{R}^2$$

where \bar{R} is given by eq. (9). Using the values of $\bar{R}/f^{1/2}$ listed in table 2 and assuming the same range of values for the tangential forces as for the perpendicular ones, we find that $\kappa_c^f \ll \kappa_c$. Hence, the Rayleigh–Taylor mode is always more unstable than the flow mode, and therefore, a melt layer which is Rayleigh–Taylor stable should also be stable under the influence of comparable tangential forces.

Acknowledgement

This work has been supported by the Office of Magnetic Fusion Energy of the US Department of Energy.

References

- [1] A.M. Hassanein, G.L. Kulcinski and W.G. Wolfer, *J. Nucl. Mater.* 103/104 (1981) 321.
- [2] A.M. Hassanein, G.L. Kulcinski and W.G. Wolfer, these proceedings.
- [3] R.R. Peterson and W.G. Wolfer, these proceedings.
- [4] K.F. Mast and H. Preis, *Proc. 11th Symp. Fusion Technology*, Oxford, UK (1980) p. 329.
- [5] S. Chandrasekhar, *Hydrodynamic and Hydromagnetic Stability* (Oxford University Press, London, 1961) Ch. 10.
- [6] R. Bellman and R.H. Pennington, *Quart. Appl. Math.* 12 (1954) 151.
- [7] S. Feldman, *J. Fluid Mech.* 6 (1959) 131.
- [8] K. Taghavi-Tafreshi and V.K. Dhir, *Int. J. Heat Mass Transfer* 23 (1980) 1433.
- [9] A.V. Grosse, *J. Inorg. Nucl. Chem.* 23 (1961) 333; *High Temp. Science* 1 (1969) 1.
- [10] L.E. Murr, *Interfacial Phenomena in Metals and Alloys* (Addison-Wesley, Reading, MA, 1975) p. 100.
- [11] T.B. Benjamin, *J. Fluid Mech.* 2 (1957) 554.